Multiple Quasi Equilibria of the ITCZ and the Origin of Monsoon Onset

WINSTON C. CHAO

Laboratory for Atmospheres, NASA Goddard Space Flight Center, Greenbelt, Maryland

(Manuscript received 30 October 1998, in final form 26 May 1999)

ABSTRACT

Supported by numerical experiment results, the abrupt change of the location of the intertropical convergence zone (ITCZ), from the equatorial trough flow regime to the monsoon trough flow regime, or the monsoon onset, is interpreted as a subcritical instability. There are two balancing ''forces'' acting on the ITCZ. One toward the equator, or an equatorial latitude depending on the convection scheme, due to the earth's rotation, has a nonlinear latitudinal dependence; and the other toward a latitude close to the sea surface temperature peak has a relatively linear latitudinal dependence. The highly nonlinear latitudinal dependence of the first ''force'' is crucial for the existence of the multiple equilibria. This work pivots on the finding that the ITCZ and Hadley circulation can still exist without the pole-to-equator gradient of radiative–convective equilibrium temperature.

The numerical experiments are done with an atmospheric general circulation model over an aquaplanet with zonally uniform sea surface temperature. The existence of the two flow regimes, the two ''forces,'' and the abrupt transition are all demonstrated in the experiments. Experimental results show high dependence on the choice of cumulus parameterization scheme, especially during the equatorial trough circulation regime. Although the proposed interpretation is more suitable for explaining the monsoon trough onset in the western Pacific, it is hypothesized that the same basic mechanism is also at the core of monsoon onset in other parts of the Tropics.

1. Introduction

Monsoon onset, the sudden arrival of rainy season after months of hot and dry weather in many parts of the Tropics, has been an age-old puzzle in geophysical fluid dynamics and tropical meteorology. It is well known that in the western Pacific the monsoon onset involves a sudden shift of the location of the intertropical convergence zone (ITCZ) as the season marches into summer from a location within 7° of the equator to a location more than 12° away from the equator (Gray 1968). The flow field associated with the ITCZ in the former location is known as the equatorial trough flow regime. That in the latter location is often referred to as the monsoon trough, well known as a favorable location for tropical cyclogenesis (Briegel and Frank 1997). The equatorial trough flow pattern is largely characterized by trade easterly converging toward the ITCZ, while the monsoon trough flow pattern is characterized by the low-level westerly wind field in the region of the ITCZ and the prominent feature of cross-equatorial low-level flow. A reverse transition occurs at the end of the summer but is usually less abrupt. Similar ITCZ transition is also observed in the Indian Ocean (the well-known Indian monsoon onset) and elsewhere in the Tropics (southeast Asia, Australia, North and South Americas, and Africa). These flow regimes and the transition between them have already been simulated using aquaplanet models (Numaguti 1995; Yano and McBride 1998) and general circulation models (GCMs) (e.g., Lau and Yang 1996). Naturally, the immediately obvious questions concerning the origin of these flow regimes, the reason for the transition between them, and the cause of the suddenness should be asked. Other intriguing questions, such as why the speed of retreat differs from that of the onset and why such transitions are not observed in the eastern Pacific, should also be raised. In this article some numerical experiments to investigate these questions are presented in the next section, and an interpretation of the results of these experiments and further supporting experiments are given in section 3. Both the experiments and the interpretation are limited to the simplified settings of aquaplanet with prescribed zonally uniform sea surface temperature (SST). The role of landmass in monsoon and its onset is not treated in this work aside from some preliminary discussions in the last section. This article is concluded with a brief summary.

2. Experiments

The model used, a 12-level atmospheric aquaplanet GCM with 4° (latitude) × 5° (longitude) grids, is essentially the same as the one used in Chao and Deng

Corresponding author address: Dr. Winston C. Chao, Mail Code 913, NASA/Goddard Space Flight Center, Greenbelt, MD 20771.
E-mail: winston.chao@gsfc.nasa.gov

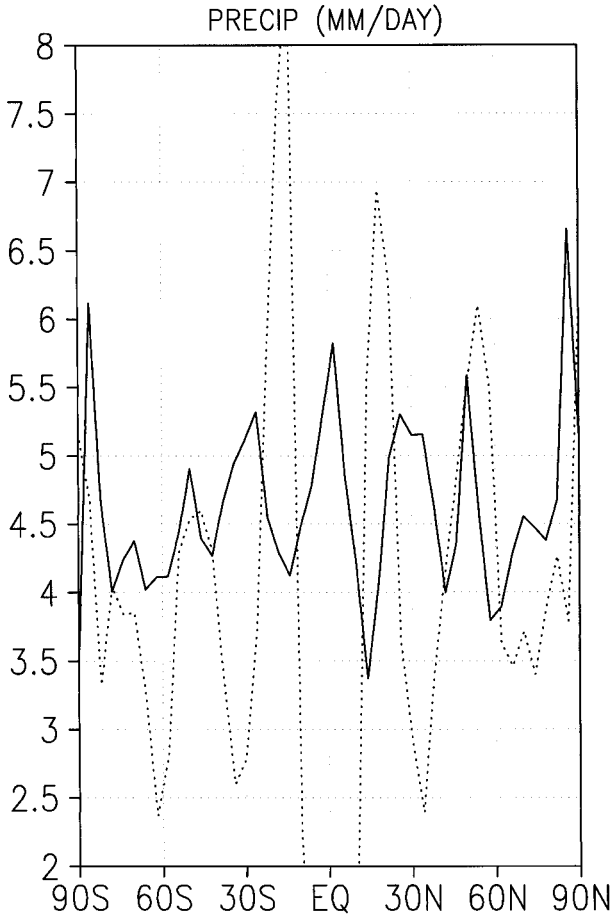

FIG. 1. Time–zonal mean precipitation of the last 60 days of a 150-day integration with constant (in time, long, and lat) SST using MCA (the solid line). The dotted line shows the result of using RAS from days 15 to 25.

(1998). The boundary layer and turbulence parameterizations are those of Louis (1979). The radiation package is that of Harshvardhan et al. (1987). To demonstrate the sensitivity of the model results to the choice of cumulus convection scheme, two cumulus parameterization schemes, the relaxed Arakawa–Schubert scheme (RAS; Moorthi and Suarez 1992) and Manabe's moist convective adjustment scheme (MCA; Manabe et al. 1965) are used. The initial condition is taken from 15 July 1981 European Centre for Medium-Range Weather Forecasts analysis interpolated to the aquaplanet setting and averaged with respect to the equator.

In order to pave way for the interpretation in the next section we did a few special experiments. The first experiment is done with a constant (in time, longitude, and latitude) SST of 302 K and a constant solar zenith angle. The solid line in Fig. 1 shows the time–zonal mean precipitation of the last 60 days of a 150-day integration with MCA. This lengthy period of integration was chosen to ensure that the initial condition has no more impact on the results. In fact, the impact of the initial condition is obvious only in the first 10 days. This experiment clearly demonstrates that the ITCZ (and the associated Hadley cells) can exist solely due to earth's rotation without any pole-to-equator gradient in radiative–convective equilibrium temperature. The high global mean precipitation value is clearly due to the high SST used throughout the globe. Figure 1 also shows precipitation belts in middle and high latitudes, presumably due to baroclinic instability, considerably different from those observed. The same experiment with RAS shows a double ITCZ averaged between days 15 and 25 (the dashed line in Fig. 1). The tendency of RAS to give double ITCZ is also obvious in the results of Chao and Deng (1998), which used higher horizontal resolution. Longer integration with RAS showed that the southern one diminished despite the symmetric-with-respect-to-equator settings, consistent with Philander et al. (1996). Similar constant SST experiments were done by Sumi (1992) and Hayashi and Golder (1997).

The next experiment is done with the true solar zenith angle, and an SST (in Kelvins) uniform in the zonal direction and varying in time and latitude according to

$$\mathrm{SST} = 273 + \Delta T \exp\{-4[(\phi - \phi_S)/L]^2\};$$
$$\phi_S = R \sin(2\pi \mathrm{day}/365), \quad (1)$$

where ϕ is the latitude in degrees, ϕ_S is the latitude of the SST peak, and R is the highest latitude in degrees that the peak of the SST can reach [day = Julian day − 74 (74 being the Julian day of 15 March); $L = 90°$; $\Delta T = 27$ K]. Thus the SST distribution is a single-peak Gaussian curve being moved according to the season. Figure 2 shows the zonally averaged precipitation in an experiment with the MCA and $R = 30°$. The global average is 4.5 mm day^{-1}, not unreasonable considering the aquaplanet setting. The results in the first 10 days, the adjusting period, can be ignored. The border of the shaded regions is a contour of 10 mm day^{-1} and the shading contour interval is 10 mm day^{-1}. The location of the SST peak is shown by the sinusoidal curve. As the SST peak moves away from the equator, the ITCZ lags it initially; and then around 10 April, when the SST peak is not yet at 15°, an onset occurs, in which the ITCZ suddenly moves closer to the SST peak but does not catch up with it. Thereafter, the poleward movement of the ITCZ again is at a much slower pace than that of the SST peak; the location of the ITCZ in fact moves very little. As the SST peak reaches 30°, the center of the ITCZ reaches only about 20°. The time–zonally averaged circulation fields (Fig. 3) during the monsoon trough period, as averaged between 1 and 6 July, exhibit low-level cross-equator meridional flow toward the ITCZ and low-level zonal mean westerlies and high-level easterlies at the latitude of the ITCZ, consistent with the observed monsoon trough circulations.

After 15 June, as the SST peak starts to move back toward the equator there is relatively little movement of the ITCZ. For a few days in August the ITCZ resides

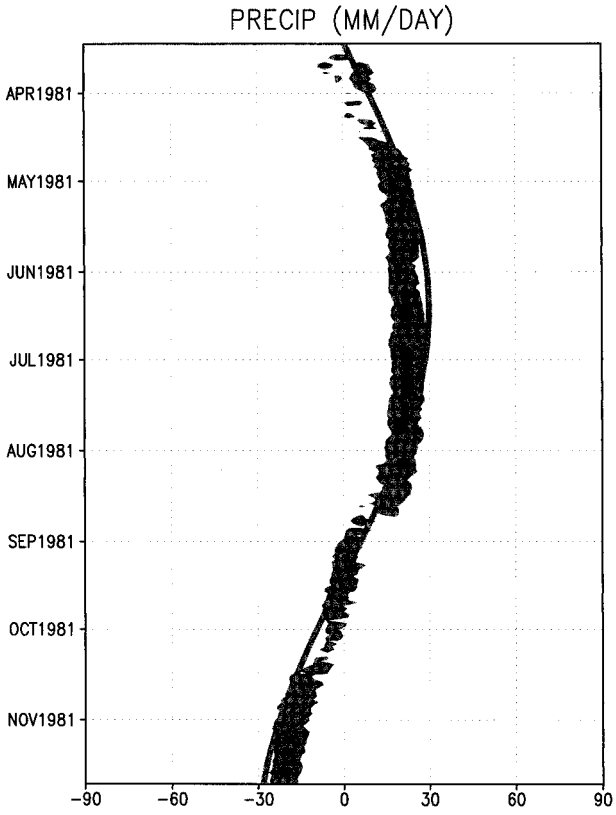

FIG. 2. Time–latitude plot of zonally averaged precipitation in an experiment with SST varying in latitude and time according to Eq. (1) and $R = 30°$. The border between the shaded and unshaded regions is a contour line of 10 mm day^{-1}. The shading contour interval is 10 mm day^{-1}. The sinusoidal line indicates the location of the SST peak.

on the poleward side of the SST peak. This is followed by a retreat starting in mid-August, which brings the ITCZ back closer to the equator. The ITCZ crosses the equator a few days after the SST peak does, apparently due to a delayed atmospheric response to the change of SST. Then between 10 and 15 October an onset occurs in the southern onset. The time of the northern onset (in April) is much earlier than that observed, resulting in a longer stay of the ITCZ in the monsoon trough regime than what is observed. [The observed SST does not vary in time and space exactly according to Eq. (1) and the model has no landmass; therefore, a detailed comparison of the onset and retreat time between the experiment and the observation is not meaningful.] This is largely due to the choice of R. A repeated experiment with $R = 20°$, shown in Fig. 4, shows a shorter stay of ITCZ in the monsoon trough regime and a longer stay in the equatorial trough regime. Also, the onset and retreat are less prominent.

Changes in the other parameters in Eq. (1) can also have a significant impact on the outcome. Changing ΔT to 31 K (R remains at 30°) virtually eliminates the onsets and renders a weak retreat with an ITCZ very much following the peak of the SST (Fig. 5). Increasing L to 180° (ΔT restored to 27 K) results in an ITCZ very close to the equator and no onset or retreat occurs (not shown). A more moderate increase of L, from 90° to 120°, gives more prominent transitions (i.e., transitions of wider latitudinal range), particularly the retreat in August (Fig. 6); correspondingly the ITCZ is closer to the equator after the retreat than it is in Fig. 2.

Figure 7 is identical to Fig. 2 except that RAS is used instead of MCA. It clearly shows sharp onset and retreat of monsoon trough in contrast to the slower transitions obtained with MCA. During the equatorial trough period, the ITCZ is considerably weaker and shows a double ITCZ structure in mid-September. In late August an equatorial ITCZ appears and soon moves into the Southern Hemisphere, and, before it disappears, a northern ITCZ appears. The northern ITCZ soon moves southward and crosses the equator as the southern onset starts. The ITCZ in the monsoon regime behaves the same as in the case of Fig. 2, in terms of the length of stay and the little change in location.

3. Interpretation and further experiments

It is heuristic to consider a simplified setting of an atmosphere over an aquaplanet with prescribed constant (in time, latitude, and longitude) SST and solar zenith angle. Thus, there is no pole-to-equator gradient in the radiative–convective equilibrium temperature, a factor long considered as a prerequisite to the atmospheric general circulation. Under such settings one might expect that convection occurred randomly, yielding uniform time mean precipitation; thus an ITCZ and the associated Hadley circulation might not occur. However, such an expectation misses an important role of the earth's rotation. Since rotation (or the Coriolis force) has an analogous behavior to stratification with slow rotation equivalent to weak stratification (Veronis 1967), the most favorable location for convection is the equator. Thus the ITCZ and Hadley circulation can still occur, as well as other circulations at higher latitudes. The characteristics of such general circulation, including the intensity and sizes of different circulation cells, may differ from the observed general circulation. Numerical experiment results using MCA shown in Fig. 1 confirm this idea and show that, besides rainbands at higher latitudes, a single ITCZ exists over the equator.

However, when MCA is replaced by RAS the ITCZ is not at the equator, a double ITCZ straddling the equator is obtained (Fig. 1) in contrast to the aforementioned expectation of the role of the Coriolis force. The resolution lies in a second role of the Coriolis force. The Coriolis force gives rise to enhanced low-level wind speed due to the low-level rotating wind component generated by the inflow toward the precipitating area. This enhanced low-level wind in turn enhances surface sensible and latent heat fluxes. This second role of the Coriolis force favors higher latitude for the location of

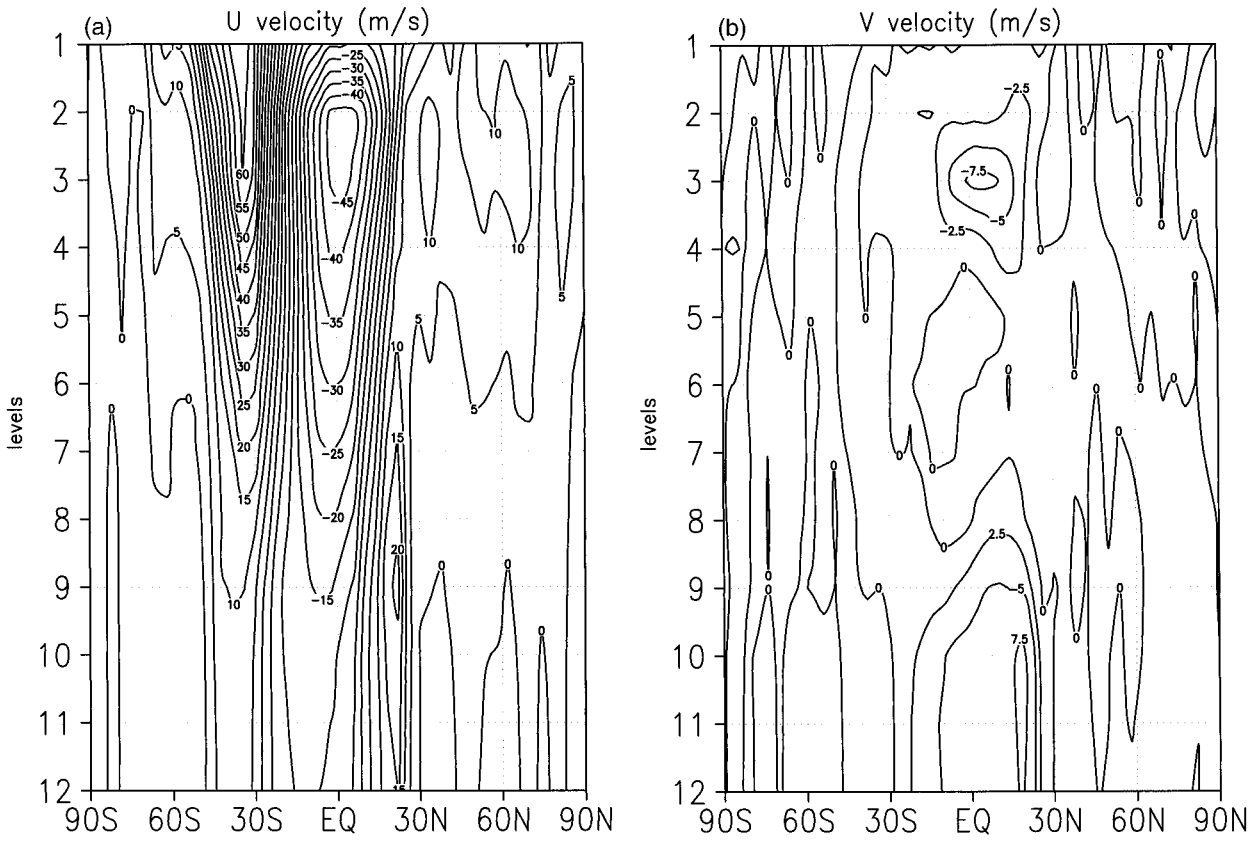

FIG. 3. Time–zonally averaged (a) zonal and (b) meridional velocities averaged between 1 and 6 Jul as a function of latitude and model levels. The pressure values of the model levels are given in Table 1 of Chao and Deng (1998). The bottom four levels are below 850 mb. The cross-equatorial low-level meridional flow and the low-level westerlies and high-level easterlies at the latitude of the ITCZ (~19°N) are the signatures of monsoonal flow.

the ITCZ. The compromise of the two opposing roles of the Coriolis force determines the location of the ITCZ. Why the second role of the Coriolis force has little weight when MCA is used is being studied and will be reported in a sequel. In the following, we will consider the MCA case first.

In a model with such aquaplanet settings, if the ITCZ is placed away from the equator initially, it will move toward the equator, its equilibrium locations, at a rate that varies with the latitude. Curve A in Fig. 8a gives a schematic of the initial acceleration rate as a function of latitude. This curve represents this acceleration or a southward ''force'' that pulls the ITCZ toward the equator as a function of latitude. This curve, of course, has a zero value at the equator; it increases (decreases) with the latitude in Northern (Southern) Hemisphere equatorial latitudes. At higher latitudes, curve A has a highly nonlinear dependence on latitude. How curve A is deduced will soon be discussed.

The movement of an ITCZ, initially set away from the equator, toward the equator (in the setting of constant SST and solar zenith angle and when MCA is used), the equilibrium location, is like that of an object tied to a weightless stretched nonlinear spring moving toward its neutral position. In such movement the object experiences a restoring ''force.'' Likewise, the ITCZ also experiences a restoring ''force.'' This ''force'' is due to earth's rotation and thus is related to the Coriolis force, but it is not the Coriolis force per se. The reason the word ''force'' is in quotes is that the ITCZ is not an object and it has no mass. The ITCZ is a flow pattern or a phase line of maximum precipitation. Thus, we cannot talk about a true force in the sense of force being equal to mass times acceleration. The movement of the ITCZ is, however, associated with an acceleration, which can be expressed mathematically as the second time derivative of the latitude of the ITCZ. The ''force'' can be defined as this acceleration. Another equivalent way of explaining the ''forces'' is that the ''forces A and B'' are the attraction experienced by the ITCZ due to the attractors at the equator and at a latitude close to that of peak SST, respectively. If one were to do an analytic study, the first step would be to derive the governing equation for the position of the ITCZ as expressed by the second time derivative of the latitude of the ITCZ being equal to an expression that reduces to curve A when the SST is uniform and to line B when rotation is set zero.

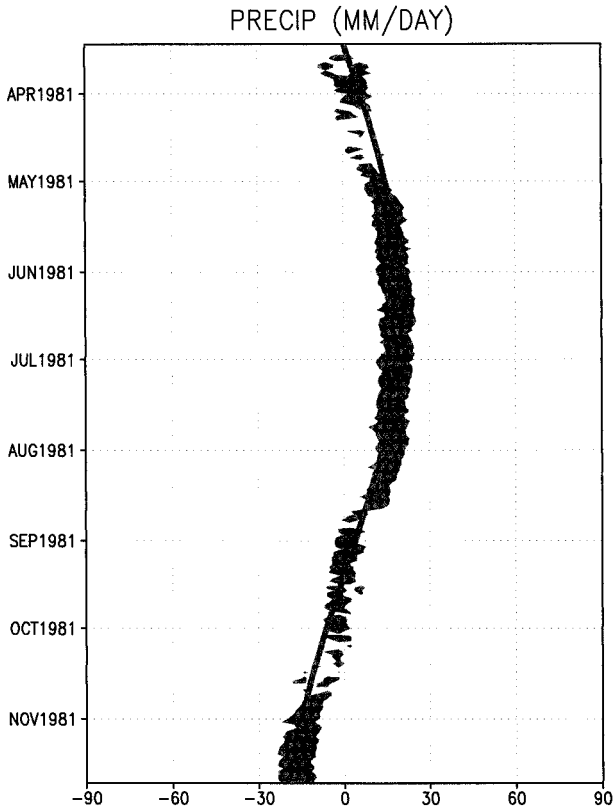

FIG. 4. Same as Fig. 2 but $R = 20°$.

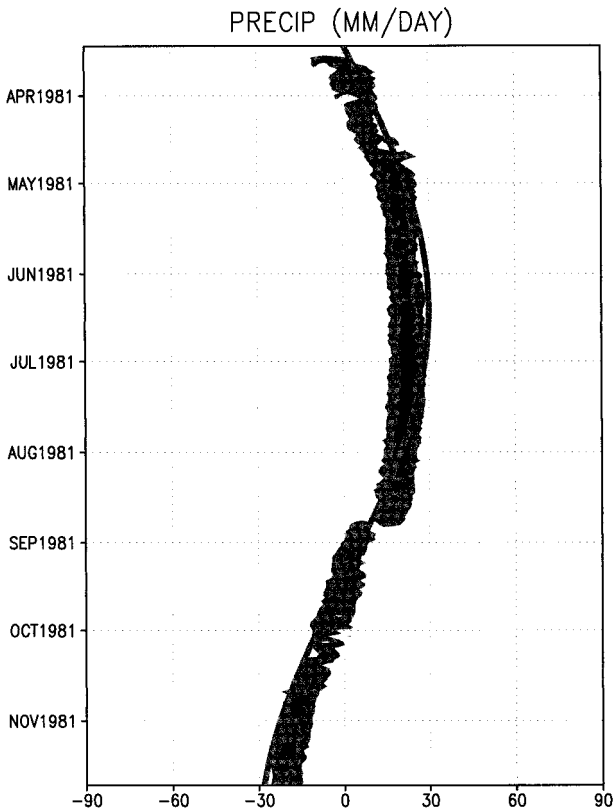

FIG. 5. Same as Fig. 2 except $\Delta T = 31$ K.

When the SST is not uniform in latitude (but does not vary in time and longitude) and when the earth does not rotate, there is a different ''force'' (positive means toward the north), which pulls the ITCZ toward a latitude, LS, very close to the latitude of maximum SST [for simplicity we assume that the SST has a single peak in latitude as in Eq. (1)], represented by line B in Fig. 8a. The exact value of LS will be determined experimentally. Without the Coriolis force the location of the ITCZ should be that of LS. Also, the magnitude of the ''force'' experienced by the ITCZ should be dependent on the distance from the maximum SST, it should have a value of zero at LS, and it is assumed that this dependence is relatively linear. For simplicity, it is further assumed that when the latitude of the maximum SST moves, line B moves with it without changing its slope (these assumptions will be discussed shortly).

The existence of the two ''forces'' can be demonstrated experimentally. Figure 9 shows an experiment similar to that of Fig. 2 except that the SST is fixed (with its peak at 30°N) after 15 June, and then on 12 September the Coriolis force is removed. It shows the ITCZ rapidly moving toward LS at 34°N in a short period; thus it clearly demonstrates the existence of the line B ''force.'' Prior to the removal of the Coriolis force the ITCZ is at an equilibrium, indicating the existence of a counterbalancing curve A ''force.''

Thus in an aquaplanet atmospheric model, if the SST is specified to vary in latitude (the effect of the solar zenith angle is minor), the location of the ITCZ is the latitude where curve A intersects line B, that is, where the two ''forces'' pulling the ITCZ toward opposite directions balance each other. When the SST has a maximum close to the equator, line B has a zero value close to the equator (e.g., line B1 in Fig. 8a) and intersects curve A at a latitude even closer to the equator. As the SST peak is moved away from the equator (as the season marches from March into April and then May), line B moves with it (at a slightly higher pace), and the ITCZ, or the abscissa of point 1 in Fig. 8a, moves also, but at a slower rate; and new intersecting points, points 2 and 3, appear. Point 2 is an unstable quasi-equilibrium state, while point 3, like point 1, is stable. As the SST peak is moved farther away from the equator, it will come to a point where point 1 disappears; thus the ITCZ moves toward the latitude of point 3, which is much closer to the location of the SST peak but still on the equator side of it. This transition is interpreted as the monsoon trough onset and is an example of subcritical instability, whose definition is given in textbooks such as Ioose and Joseph (1980). The speed of this transition far outstrips the speed that the ITCZ assumes when moving from the equator to the latitude of point 1 just before point 1 vanishes. The former speed is that of a ''free-fall'' ac-

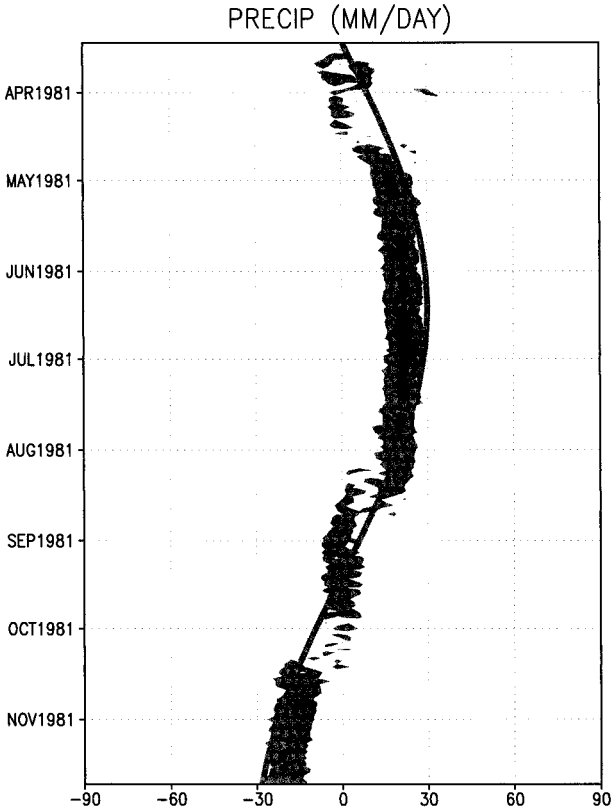

FIG. 6. Same as Fig. 2 except $L = 120°$. The border between the shaded and unshaded regions is a contour line of 8 mm day^{-1}. The shading contour interval is 8 mm day^{-1}.

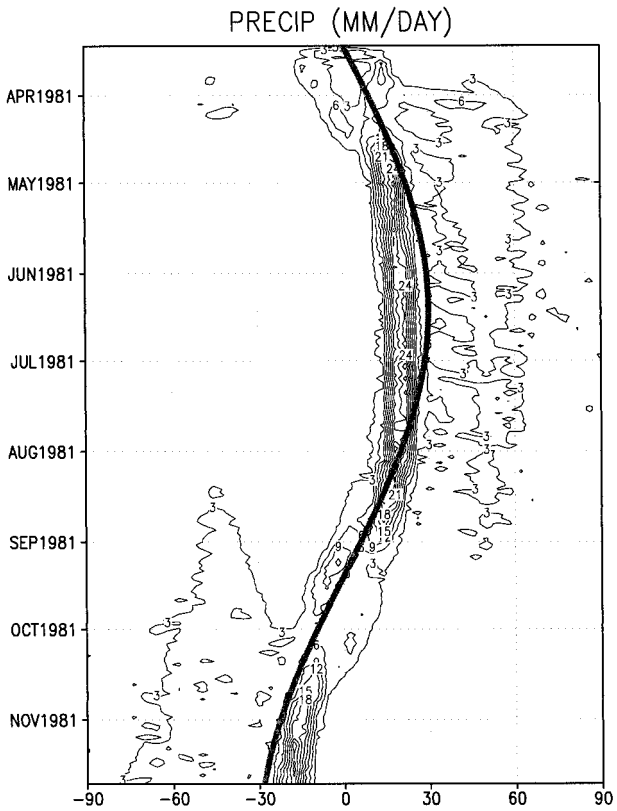

FIG. 7. Same as Fig. 2 except that RAS is used instead of MCA. The contour lines are 3, 6, 9, 12, 18, and 30 mm day^{-1}.

celerated by the difference between curve A and line B, and the latter speed lags the seasonal march of maximum SST. This explains the suddenness of the monsoon trough onset. This free-fall toward point 3, according to Fig. 8a, might not just stop at point 3. The flow state could overshoot point 3 and then bounce back, resulting in an oscillation about point 3. The fact that both observation and our experimental results do not show any oscillation in latitude of the ITCZ (beyond the normal fluctuation within the realm of quasi-equilibrium state of the monsoon ITCZ) during the onset indicates that the damping effect (not shown in Fig. 8a), where its size is related to the speed of the ITCZ moving toward point 3 (as in a damped oscillator), is sizable enough to prevent an oscillation around the new latitudinal location.

On the return trip, as the SST peak moves back toward the equator, line B moves toward the equator and points 1 and 2 reappear; but the state of the atmosphere is still that of point 3 even after passing the onset point, until point 3 eventually disappears and then the state jumps back to point 1. This jump, identified as the retreat of monsoon trough, covers a different latitudinal range, and the associated accumulated ''force,'' as represented by the area of the light shaded region in Fig. 8b, is different from that of onset represented by the area of the dark shaded region. This difference contributes to the difference between the speed of the onset and that of the retreat. Notice that the light shaded area is larger than that of the dark shaded area in Fig. 8b, consistent with the retreat being more prominent than the onset in Figs. 2, 4, 5, and 6. Besides, the damping effect experienced during the transition may have latitudinal dependence. The round-trip results in a hysteresis loop in the 2D space spanned by the latitude of the ITCZ and the peak latitude of the SST. In this theory line B does not have to be exactly linear. It would suffice if line B had a magnitude that were an increasing function of the latitudinal distance between the ITCZ and the SST peak and if it reached a maximum larger than the maximum of curve A within the Tropics. Perhaps the most crucial part of this interpretation is the shape of curve A (here the shape of curve A includes the rising from the equator, the subsequent decline, and the next rising poleward of 17°N), which makes the multiple equilibria possible and thus explains the existence of the onset and retreat.

At this point, a discussion is in order on how the dependence of curve A on the latitude, or the shape of curve A, is determined. Figure 10 is a repeat of Fig. 2 except that, instead of a sinusoidal seasonal change of the location of SST peak, the SST peak moves linearly in time from equator to 30°N (also the solar angle from

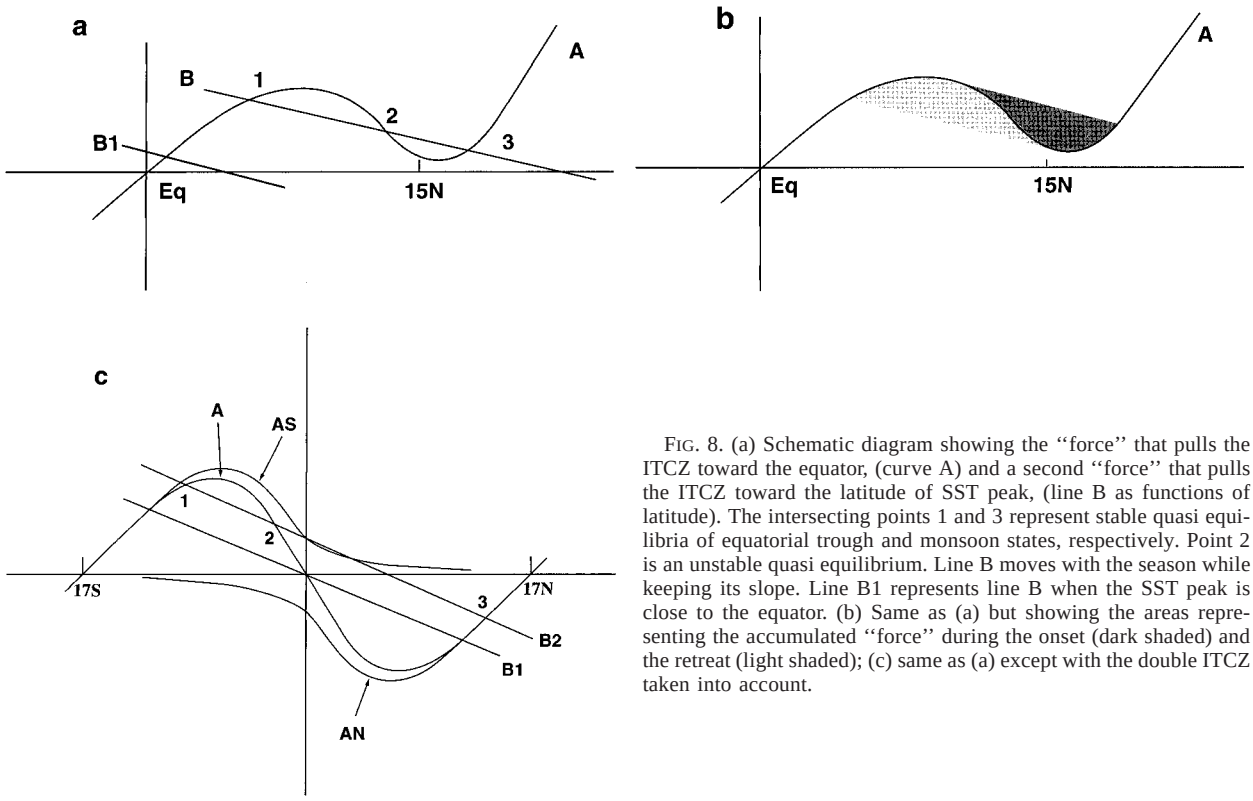

FIG. 8. (a) Schematic diagram showing the ''force'' that pulls the ITCZ toward the equator, (curve A) and a second ''force'' that pulls the ITCZ toward the latitude of SST peak, (line B as functions of latitude). The intersecting points 1 and 3 represent stable quasi equilibria of equatorial trough and monsoon states, respectively. Point 2 is an unstable quasi equilibrium. Line B moves with the season while keeping its slope. Line B1 represents line B when the SST peak is close to the equator. (b) Same as (a) but showing the areas representing the accumulated ''force'' during the onset (dark shaded) and the retreat (light shaded); (c) same as (a) except with the double ITCZ taken into account.

equinox to solstice) in 276 days; thus the rate of northward movement of the SST peak (indicated by the thin straight line) is much slower than (about one-third of) that in Fig. 2. Figure 11 is the same as Fig. 10 except that the Coriolis force is removed; that is, it shows LS (the latitude at which line B intersects the x axis in Fig. 8) as the SST peak changes. Assuming that the slope of line B does not have significant change when the SST peak moves from the equator to 30°N (this assumption will be discussed shortly), the shape of curve A can be obtained by the location of the SST peak and that of the ITCZ by noting that curve A intersects line B at the latitude of the ITCZ. Figures 10 and 11 show that as the SST peak leaves the equator, the ITCZ follows LS at a slower speed. This indicates that curve A has a positive slope close to the equator (as expected from the constant SST experiment). Between 7° and 17°N the ITCZ moves at a speed higher than that of LS. This indicates a negative slope of curve A between these latitudes. In the neighborhood of 17°N the ITCZ is very close to LS, indicating that curve A drops to a low point in this region. Northward of 17°N, Fig. 10 again shows a slower rate of change of the ITCZ location than that of the LS, indicating a positive slope of curve A north of 17°N. Judging from the fact that, in Fig. 11, north of 17°N the ITCZ location changes at a slower rate than it does near the equator, one can state that the slope of curve A is greater north of 17°N than near the equator (Fig. 8a). The fact that Fig. 10 shows no sign of onset only indicates a large (absolute) slope of line B such that no multiple equilibria can occur. In Fig. 2 since the SST moves at much higher speed (than in Fig. 10), the atmosphere feels an effective Gaussian SST distribution with much lower amplitude, which is equivalent to a smaller (absolute) slope for line B. Such smaller (absolute) slope of line B generates multiple equilibria. This same reason also accounts for the difference between Fig. 2 ($R = 30°$) and Fig. 4 ($R = 20°$). In Fig. 4 since the SST peak moves slower, the effective (absolute) slope of line B is larger, resulting in less prominent onset and retreat and a shorter stay in the monsoon trough regime. The origin of the shape of curve A will be explained in a sequel.

It should be emphasized that the intersecting points in Fig. 8a do not represent a fixed-point (or steady state) solution. Instead, they represent quasi-equilibrium states. Factors making these states nonsteady [e.g., Schubert et al. (1991)] are not included in Fig. 8a. Notice that in all figures the ITCZ has short-term (less than 5 days) fluctuations.

Our interpretation can explain many of the findings in the numerical experiments presented in the last section. Besides providing an explanation for the origin of the two flow regimes and the transition between them, it also explains why the ITCZ always stays on the equatorial side of the SST peak until the retreat. Figure 2 shows that ITCZ remains on the equatorial side of the SST peak, and as the SST peak moves poleward, the

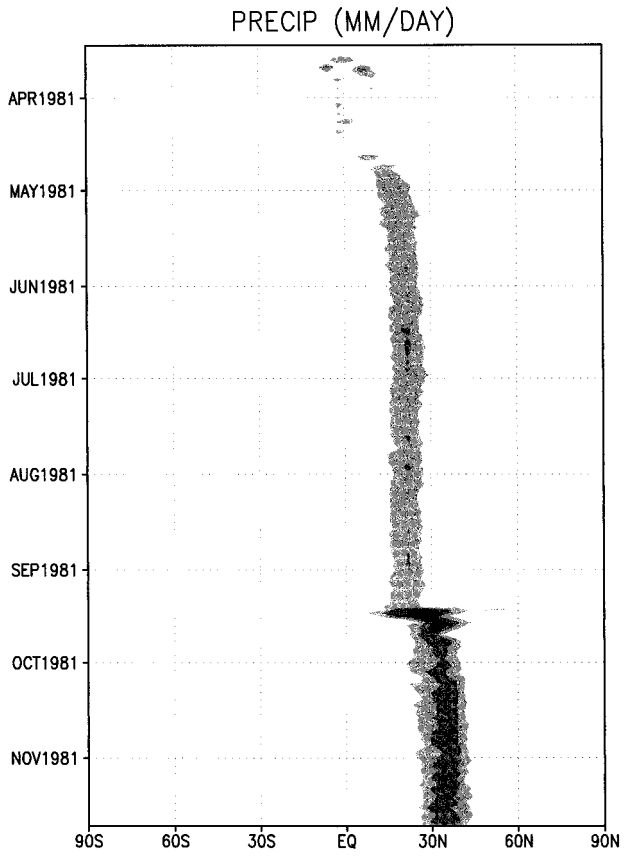

FIG. 9. Same as Fig. 2 except that the SST is fixed after 15 Jun, and then on 12 Sep the Coriolis force is removed.

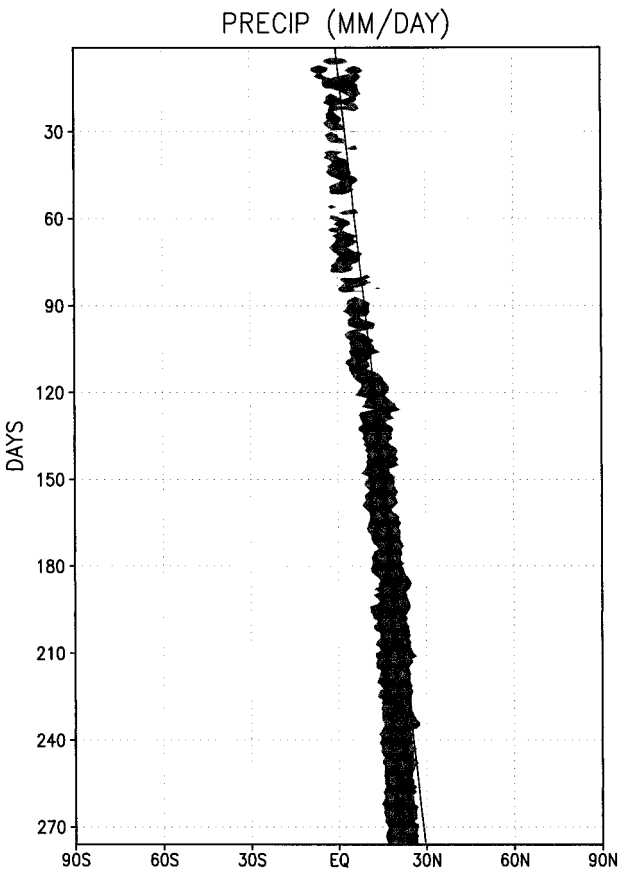

FIG. 10. Same as Fig. 2 except that the SST peak moves linearly in time from equator to 30°N in 276 days. The thin straight line indicates the location of the SST peak.

ITCZ moves at a slower speed until the transition occurs in agreement with our theory. Increasing ΔT has the effect of increasing the SST control of the ITCZ, or equivalently steepening the (absolute) slope of line B, which according to Fig. 8a, shortens the distance between points 1 and 3. Further increase of ΔT leads to the elimination of the multiple equilibria. This was obtained in the experiment associated with Fig. 5. Doubling L (from 90° to 180°), or reducing ΔT, would mean a weak SST peak or a very small (absolute) slope of line B, resulting in an ITCZ close to the equator year round. Thus no transition can occur. This explains the nonexistence of monsoon trough onset in the eastern Pacific, where the SST peak is weaker than that in the western Pacific. A more modest increase of L, from 90° to 120°, implies a greater distance between points 1 and 3 in Fig. 8a. This leads to more prominent transitions as demonstrated in the experiment associated with Fig. 6. Also, Fig. 6 gives an earlier retreat than Fig. 2, as expected from Fig. 8a when line B has a smaller (absolute) slope.

Our interpretation does not require that line B be exactly linear. As long as line B reaches a peak higher than the peak of curve A, onset can occur. This, of course, can be achieved by prescribing a large enough amplitude and a broad enough size to the SST peak (as we have already done in the experiments). Noting that the location LS can be considered as an attractor, one can expect that line B in its entirety has the shape of curve A in Fig. 8c enlarged and stretched in the north–south direction, and for simplicity we have only drawn in Fig. 8 its portion close to LS. The assumption that the slope of line B does not change when the SST peak moves is not a strict one; a certain amount of change does not affect our argument. Although we do not have rigorous argument based on fundamental principles for this assumption, the experiment results lend support to this assumption in the sense that they are consistent with our arguments when this assumption is made.

Figure 7, using RAS, presents results that are considerably different from Fig. 2. These results can be interpreted in a similar manner. Curve A is now the sum of two curves (Fig. 8c), AN and AS; each is related to one ITCZ, again based on the attractor concept. Each curve has a zero value at the location of the corresponding ITCZ in Fig. 1. This is supported by Fig. 12, the counterpart of Fig. 10. Figure 12 shows a weak double ITCZ about 13° apart between days 20 and 30, and the southern one soon diminishes and appears to jump to-

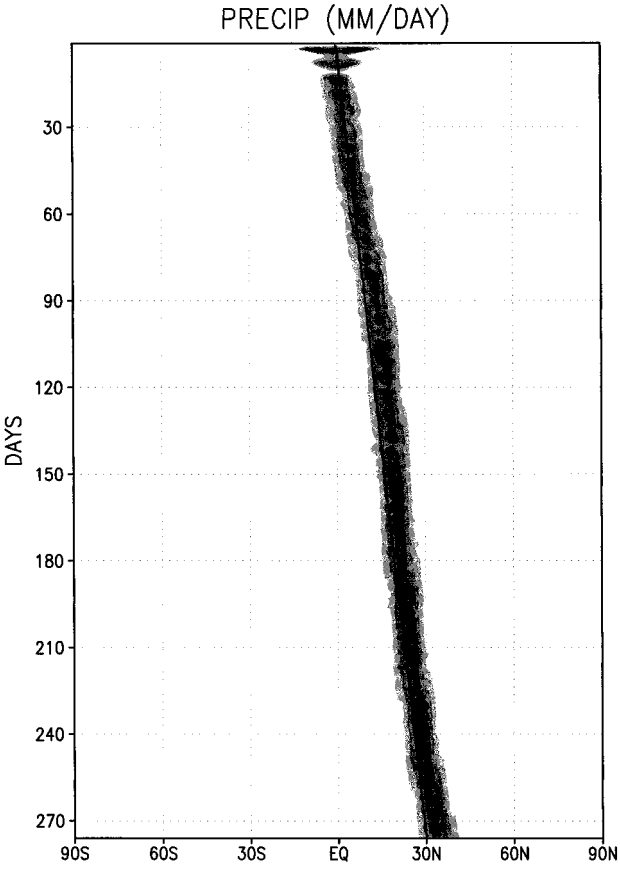

FIG. 11. Same as Fig. 10 except that the Coriolis force is removed.

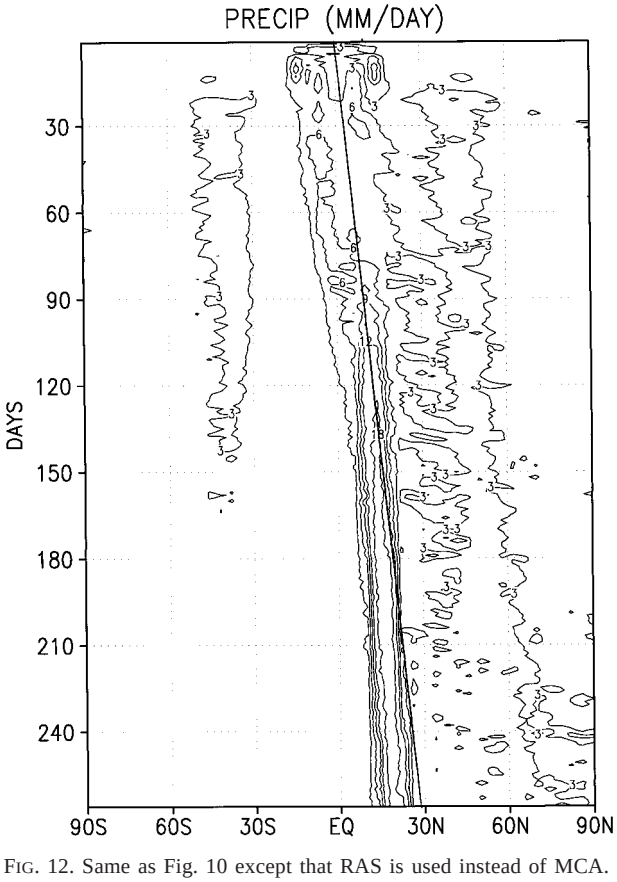

FIG. 12. Same as Fig. 10 except that RAS is used instead of MCA.

ward and cross the equator, moving to the poleward side of the SST peak. After day 70 the ITCZ becomes well established in strength. Its poleward movement is much slower than that of the SST peak, indicating a positive slope for curve AN. When the SST peak reaches 15°N the ITCZ crosses it, indicating the zero value of curve AN at 15°N. Thereafter, the positive slope of curve AN remains. Without SST gradient, that is, if line B does not exist in Fig. 8c, the two ITCZs (at the intersecting points of the two curves with the horizontal axis in Fig. 8c) are far apart, as shown in Fig. 1. When an SST profile symmetric with respect to the equator is present and when the SST peak becomes stronger, line B (B1 in Fig. 8c) intersects the horizontal axis at the equator and gains in slope, thus drawing closer the two ITCZs (points where line B1 intersects the two curve A's). Notice that the two ITCZs are about 35° apart in Fig. 1 and are only about 15° apart on 19 September in Fig. 7. If the SST peak is increased further, it will come to a point where the (absolute) slope of line B becomes greater than that of curve A, so that the double ITCZ will suddenly merge into a single ITCZ. Figure 13 shows such an experiment with RAS in which the SST follows Eq. (1) except that its peak remains at the equator and L is reduced from 90° to 60° in 136 days. Notice that after a period of strength fluctuation between the two ITCZs from day 60 to day 90 the double ITCZ merges into a single ITCZ, which then gains in strength due to the increasing sharpness of the SST peak.

Next, when the SST peak moves southward toward the equator as the season marches on, the single ITCZ (point 3 on curve A) moves equatorward also (Fig. 8c) at a lower speed, and eventually new intersecting points (points 1 and 2) appear. At this time a new ITCZ (corresponding to point 1 of Fig. 8c) appears in the Southern Hemisphere (Fig. 7). It grows at the expense of the northern (point 3) ITCZ. The new one appears before the existing one vanishes, in contrast to the MCA experiments where movement from the just-vanished old position to a new one is the rule. The reason for this difference is not clear at this point. The northern ITCZ (corresponding to point 3) soon disappears, though point 3 still exists. After the SST peak crosses the equator, point 3 becomes closer to the equator; thus the ITCZ corresponding to it reappears and at the same time the point 1 ITCZ weakens. As the SST peak moves farther into the Southern Hemisphere, point 3 disappears and the point 1 ITCZ located on the poleward side of the SST peak becomes the only ITCZ. After the SST peak moves southward of 15°S, the ITCZ resides on the equatorward side of the SST peak. These sequence of events

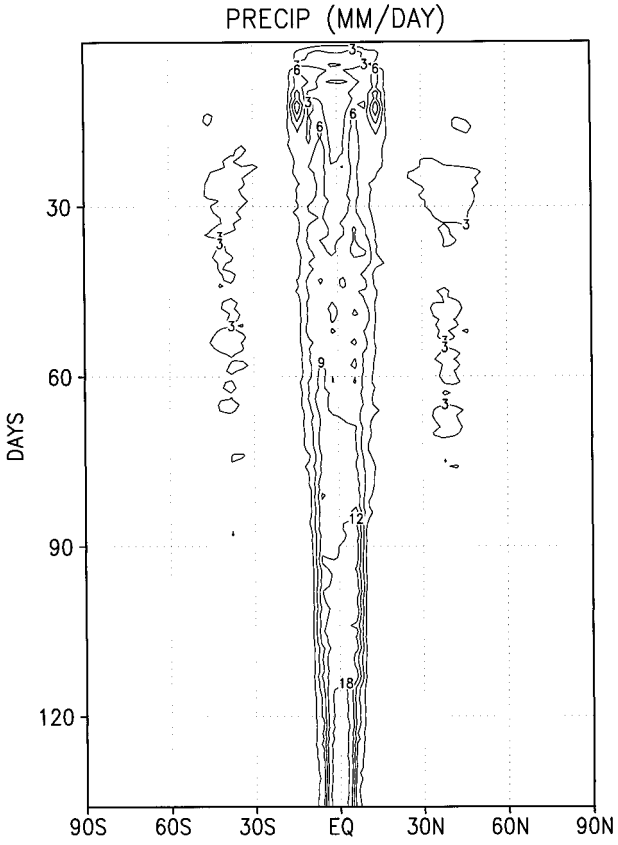

FIG. 13. Same as Fig. 7 except that the SST peak remains at the equator and L changes from 90° to 60° in 136 days.

are shown in Fig. 7. Similar numerical results were obtained by Numaguti (1995, his Fig. 20) using the Arakawa–Schubert scheme.

4. Remarks and summary

It would be highly desirable if curve A and line B were derived analytically. Unfortunately, the task of formulating a cumulus parameterization scheme simple enough to make such a derivation possible remains formidable, not to mention the other highly nonlinear aspects of the problem.

Our results can also be used to interpret one important aspect of Yano and McBride (1998); that is, in general, the latitude of the SST peak at the time of the transition decreases as the magnitude of the SST perturbation (in latitude) increases. This corresponds to an increase of the (absolute) slope of line B in Fig. 8a.

Additional numerical experiments using prescribed net radiative cooling rate (replacing the radiation package) have demonstrated that convective–radiative interaction is not an important factor for onset to occur. Nevertheless, the modifying role of the convective–radiative interaction cannot be totally ignored.

Although we have used an aquaplanet setting to explain the origin of monsoon trough onset, it is easy to understand that with the real land–sea distribution the rapid heating up of the land, say India, in the premonsoon season can partially take the place of the northward movement of the SST peak that we have used in the model. However, the role of the heating up of the land in India should not be overemphasized. India is surrounded on two sides by seas of larger areas than itself. Also note that the Indian monsoon depressions are mostly initiated over the ocean. The long-held belief that monsoon circulation has to do with land–sea contrast on a continental or subcontinental scale is not being challenged here. Once the onset process has taken place, the land–sea contrast is important in determining the monsoon flow pattern. Our hypothesis is that the monsoon onset process in India is not fundamentally different from the monsoon trough onset process in the western Pacific; both are characterized by a sudden jump of the ITCZ (Fig. 10 of Lau and Yang 1996). Also our aquaplanet simulations do capture the two important signatures of monsoon flow as stated in the discussion above associated with Fig. 3. These two signatures are found both in the Indian monsoon and in the western Pacific monsoon trough. Land–sea contrast is important in modifying the monsoon flow pattern once the onset process has taken place. The time mean low-level cross-equatorial flow changes from being uniform in longitude for the aquaplanet monsoon to being concentrated in the western Indian Ocean for the Indian monsoon. Figure 7.6 of James (1994) gives such a discussion; in his Fig. 7.6a, the cross-equatorial flow can be induced by an SST peak (instead of a hot continent) north of the equator. Moreover, the land–sea distribution (and the longitudinal variation of SST) will bring about the different monsoon onset time at different longitudes. We must emphasize that our discussion on the role of landmass has been somewhat speculative; this is a topic worthy of further research.

Being a subcritical instability, the monsoon onset bears more than a passing resemblance to stratospheric sudden warming (Chao 1985), blocking onset (Charney and DeVore 1979; Rex 1950), and polar icecap instability (Ghil and Childress 1987); they all involve sudden transition between quasi equilibria. However, it should be mentioned that their dynamics are fundamentally different.

Finally, the large difference between experiments using RAS and those using MCA indicates that the choice of the cumulus parameterization scheme is crucial. The differences are particularly prominent during the equatorial trough flow regime. The implication for coupled atmospheric–oceanic modeling, where good surface wind simulation is crucial, is clear. Thus these differences point to the importance of more research in cumulus parameterization in the context of interaction between convection and large-scale circulation. Furthermore, the successful forecast of monsoon onset and re-

treat events presents a good contest among various cumulus parameterization schemes.

In summary, the abrupt transition between monsoon trough and equatorial trough in the western Pacific is interpreted as a subcritical instability. There are two balancing ''forces'' acting on the ITCZ. One toward the equator, or an equatorial latitude depending on the cumulus parameterization scheme, due to the earth's rotation, has a nonlinear latitudinal dependence; and the other toward a latitude close to that of the sea surface (or ground) temperature peak has a relatively linear latitudinal dependence. The highly nonlinear latitudinal dependence of the first ''force'' is crucial for the existence of the multiple equilibria. Numerical simulation experiments with an aquaplanet model support this interpretation. Experimental results show high dependence on the choice of cumulus parameterization scheme, especially during the equatorial trough circulation regime. Although the proposed interpretation is more suitable for explaining monsoon onset in the western Pacific, it is hypothesized that the same mechanism is also at the core of monsoon onset in other parts of the Tropics.

Acknowledgments. Most of this work was done during a period when the author was a part-time visitor at the National Centers for Environmental Prediction. The author thanks Dr. Eugenia Kalnay, now at UMD, for her hospitality. Thanks are also extended to Dr. Song-You Hong of NCEP for his help in brushing up the author's computer skills. Drs. Wesley Ebisuzaki and Wayne Higgins of NCEP and Dr. Baode Chen and Mr. Greg Walker of Goddard gave the author helpful tips on computer graphics. This work was supported by NASA/Earth Science Division with funds managed by Drs. Kenneth Bergman and Ramesh Kakar.

REFERENCES

Briegel, L. M., and W. M. Frank, 1997: Large-scale influence on tropical cyclogenesis in the western north Pacific. *Mon. Wea. Rev.,* **125,** 1397–1413.

Chao, W. C., 1985: Stratospheric sudden warmings as catastrophes. *J. Atmos. Sci.,* **42,** 1631–1646.

——, and L. Deng, 1998: Tropical intraseasonal oscillation, super cloud clusters, and cumulus convection schemes. Part II: 3D Aqua-planet simulations. *J. Atmos. Sci.,* **55,** 690–709.

Charney, J. G., and J. G. DeVore, 1979: Multiple flow equilibria in the atmosphere and blocking. *J. Atmos. Sci.,* **36,** 1205–1216.

Ghil, M., and S. Childress, 1987: *Topics in Geophysical Fluid Dynamics: Atmospheric Dynamics, Dynamo Theory, and Climate Dynamics.* Springer-Verlag, 485 pp.

Gray, W. M., 1968: Global view of the origin of tropical disturbances and storms. *Mon. Wea. Rev.*, **96,** 669–700.

Harshvardhan, R. Davis, D. A. Randall, and T. G. Corsetti, 1987: A fast radiation parameterization for general circulation models. *J. Geophys. Res.*, **92,** 1009–1016.

Hayashi, Y., and D. G. Golder, 1997: United mechanisms for the generation of low- and high-frequency tropical waves. Part I: Control experiments with moist convective adjustment. *J. Atmos. Sci.,* **54,** 1262–1276.

Iooss, G., and D. D. Joseph, 1980: *Elementary Stability and Bifurcation Theory.* Springer-Verlag, 286 pp.

James, I. N., 1994: *Introduction to Circulating Atmospheres.* Cambridge University Press, 422 pp.

Lau, K.-M., and S. Yang, 1996: Seasonal variation, abrupt transition, and intraseasonal variability associated with the Asian summer monsoon in the GLA GCM. *J. Climate,* **9,** 965–985.

Louis, J.-F., 1979: A parametric model of vertical eddy fluxes in the atmosphere. *Bound.-Layer Meteor.*, **17,** 187–202.

Manabe, S., J. Smagorinsky, and R. F. Strickler, 1965: Simulated climatology of a general circulation model with a hydrological cycle. *Mon. Wea. Rev.,* **93,** 769–798.

Moorthi, S., and M. J. Suarez, 1992: Relaxed Arakawa–Schubert: A parameterization of moist convection for general circulation models. *Mon. Wea. Rev.,* **120,** 978–1002.

Numaguti, A., 1995: Dynamics and energy balance of the Hadley circulation and the tropical precipitation zones. Part II: Sensitivity of meridional SST distribution. *J. Atmos. Sci.,* **52,** 1128–1141.

Philander, S. G. H., D. Gu, D. Halrpen, G. Lambert, N.-C. Lau, T. Li, and R. C. Pacanowski, 1996: Why the ITCZ is mostly north of the equator. *J. Climate,* **9,** 2958–2972.

Rex, D. F., 1950: Blocking action in the middle troposphere and its effect upon regional climate: I. An aerological study of blocking action. *Tellus,* **2,** 196–211.

Schubert, W. H., P. E. Ciesielski, D. E. Stevens, and H.-C. Kuo, 1991: Potential vorticity modeling of the ITCZ and the Hadley circulation. *J. Atmos. Sci.,* **48,** 1493–1509.

Sumi, A., 1992: Pattern formation of convective activity over the aqua-planet with globally uniform sea surface temperature. *J. Meteor. Soc. Japan,* **70,** 855–876.

Veronis, G., 1967: Analogous behavior of rotating and stratified fluids. *Tellus,* **19,** 620–633.

Yano, J. I., and J. L. McBride, 1998: An aquaplanet monsoon. *J. Atmos. Sci.,* **55,** 1373–1399.